

Optical Engineering

OpticalEngineering.SPIEDigitalLibrary.org

Determination of external quantum efficiency in semiconductors using pulsed power-dependent photoluminescence

Chengao Wang
Mansoor Sheik-Bahae

SPIE.

Chengao Wang, Mansoor Sheik-Bahae, "Determination of external quantum efficiency in semiconductors using pulsed power-dependent photoluminescence," *Opt. Eng.* **56**(1), 011106 (2016), doi: 10.1117/1.OE.56.1.011106.

Determination of external quantum efficiency in semiconductors using pulsed power-dependent photoluminescence

Chengao Wang* and Mansoor Sheik-Bahae

University of New Mexico, Department of Physics and Astronomy, Optical Science and Engineering Program, 1919 Lomas Boulevard Northeast, Albuquerque, New Mexico 87131, United States

Abstract. External quantum efficiency (EQE) is a parameter widely used in various photonic devices. In laser refrigeration of solids, materials with high EQE are essential for achieving net cooling. Pulsed power-dependent photoluminescence measurement is developed and demonstrated to be a rapid and efficient tool to determine the EQE and screen the sample quality before the fabrication process for the application of laser cooling in semiconductors. EQE values obtained from this technique are shown to be consistent with results from other more precise, but time-consuming measurements for various samples at different temperatures. © 2016 Society of Photo-Optical Instrumentation Engineers (SPIE) [DOI: 10.1117/1.OE.56.1.011106]

Keywords: external quantum efficiency; laser cooling of semiconductors; photoluminescence.

Paper 161067SSP received Jul. 5, 2016; accepted for publication Sep. 13, 2016; published online Oct. 5, 2016.

1 Introduction

External quantum efficiency (EQE or η_{ext}) is an important parameter that characterizes many photonic devices. To clarify, two different definitions of EQE are used historically. The first one is used exclusively in solar cells and defined as the ratio of the number of charge carriers collected by the solar cell to the number of photons of a given energy shining on the solar cell from outside. The second and more widely used definition of EQE is a coefficient that accounts for both the efficiency of the photon–electron conversion process (internal quantum efficiency) and the efficiency of moving light into and/or out of the device (coupling efficiency). These are two different concepts and should not be confused. In this paper, we discuss EQE in terms of the second definition.

EQE is widely used to evaluate light emitting diodes, photovoltaics,¹ semiconductor lasers, and emerging technology such as laser-induced refrigeration of solids.² In photovoltaics, EQE is a measure of the available open-circuit voltage and high EQE is a necessity for approaching the Shockley–Queisser efficiency limit.¹ In laser refrigeration of solids, EQE is a critical parameter and net cooling can only be achieved in samples with very high EQE.

Laser cooling in rare-earth-doped solids was first demonstrated in 1995³ and a cryogenic temperature was recently achieved.^{4,5} Laser cooling in semiconductors is more appealing because of its much lower achievable temperatures and the possibility for integration into electronics and other photonic devices.⁶ The first demonstration of laser cooling in semiconductors was reported in 2013 on cadmium sulfide nanobelts.⁷ However, net cooling in bulk semiconductor materials remain elusive despite the ultrahigh EQE value reported.⁸ A precise and rapid measurement of EQE for cooling samples is an important step for understanding the material property and ultimately achieving net cooling.

Nevertheless, precise measurement of EQE becomes increasingly difficult when it is approaching unity, as for the samples for laser cooling. Measurement of EQE in semiconductors is particularly challenging since it is carrier density dependent.

2 Theory

For an intrinsic semiconductor, the recombination of photo-generated electron–hole pairs (N) is conveniently written as the sum of the nonradiative (AN), radiative (BN^2), and Auger (CN^3) processes, where A , B , and C are the corresponding decay coefficients.⁶ This defines the internal quantum efficiency

$$\eta_{\text{int}} = \frac{BN^2}{AN + BN^2 + CN^3}. \quad (1)$$

The luminescence extraction efficiency (η_e) accounts for radiation trapping and reabsorption (i.e., photon recycling), which limits the amount of luminescence that exits the semiconductor. This luminescence trapping essentially manifests itself as inhibiting the spontaneous emission by modifying B to $\eta_e B$. We define EQE (η_{ext}) as the fraction of photogenerated electron–hole pairs that appear as luminescence photons outside the structure²

$$\eta_{\text{ext}} = \frac{\eta_e BN^2}{AN + \eta_e BN^2 + CN^3}. \quad (2)$$

Various techniques have been developed to measure EQE in semiconductor materials.^{9–14} Most recently, researchers at the University of New Mexico show that wavelength-dependent temperature change can be used to directly measure the EQE of a semiconductor photonic device.¹⁴ This approach, called all-optical scanning laser calorimetry (ASLC)

*Address all correspondence to: Chengao Wang, E-mail: puffwang@unm.edu

or laser-induced temperature modulation spectrum (LITMoS), measures EQE with precisions of $\pm 0.1\%$ and has been effective for characterizing both semiconductor materials and rare-earth-doped solids for laser refrigeration applications.^{4,14} The only drawback of this technique is that it is very time-consuming as it requires a very precise temperature measurement and is thus restricted by the thermal relaxation time of the sample. In order to screen the samples quickly for potential cooling candidates, a rapid measurement of EQE is desired and the precision requirement can be relaxed. For this purpose, they show that power-dependent photoluminescence (PDPL) measurement can be a very useful tool because it makes it possible to determine EQE in a fast manner without implementing the time-consuming ASLC measurement and before the complicated sample fabrication.^{14,15} However, temperature change of the sample was an issue in all previous PDPL experiments as a continuous-wave (CW) laser was used as the pump source. The temperature change will then alter luminescence intensity, distorting the PDPL data. Here, we modify the previous PDPL experiment by using a pulsed laser source, which will create as much carrier density as the CW laser but will generate much less heat. We call this a pulsed-PDPL experiment.

The analytical expression of pulsed-PDPL can be derived from the rate equation subject to an impulsively injected initial carrier density N_0 .⁶

$$\frac{dN}{dt} = -(AN + \eta_e BN^2 + CN^3). \quad (3)$$

Rewrite the rate equation in the form

$$\left[\frac{1}{N} - \frac{N+q}{(N-s_1)(N-s_2)} \right] dN = -Adt, \quad (4)$$

where $q = B/C$, $s_{1,2} = [(-B \pm \sqrt{B^2 - 4AC})/2C] = N^{\text{opt}} \left\{ \left[-1 \pm \sqrt{1 - (1 - \eta_{\text{ext}}^{\text{opt}})^2} \right] / (1 - \eta_{\text{ext}}^{\text{opt}}) \right\}$, and $\eta_{\text{ext}}^{\text{opt}} \approx [1 - (2\sqrt{AC}/\eta_e B)]$ is the maximum EQE when carrier density is optimized at $N^{\text{opt}} = \sqrt{A/C}$.

The solution of the differential equation [Eq. (4)] is given by the following transcendental equation:

$$n(t) \left(\frac{1 + \frac{\sigma_1}{\varphi}}{n + \frac{\sigma_1}{\varphi}} \right)^{v_1} \left(\frac{1 + \frac{\sigma_2}{\varphi}}{n + \frac{\sigma_2}{\varphi}} \right)^{v_2} = \exp^{-At}, \quad (5)$$

where we define normalized carrier density $n(t) = N(t)/N_0$, $\sigma_{1,2} = (-s_{1,2}/N^{\text{opt}})$, $v_1 = [-\sigma_2/(\sigma_1 - \sigma_2)]$, $v_2 = [-\sigma_1/(\sigma_2 - \sigma_1)]$, and $\varphi = (N_0/N^{\text{opt}})$, with N_0 denoting the initial carrier density at $t = 0$.

Equation (5) gives the carrier density N as a function of t . We can then obtain the luminescence power by

$$P_{\text{lum}} = h\tilde{\nu}_f \eta_e \int BN(t)^2 dt \propto \int n(t)^2 dt. \quad (6)$$

where $\tilde{\nu}_f$ is the escaped (i.e., measured) mean luminescence frequency.⁶

Here, we have assumed that the incident pulse is instantaneous (delta function), thus

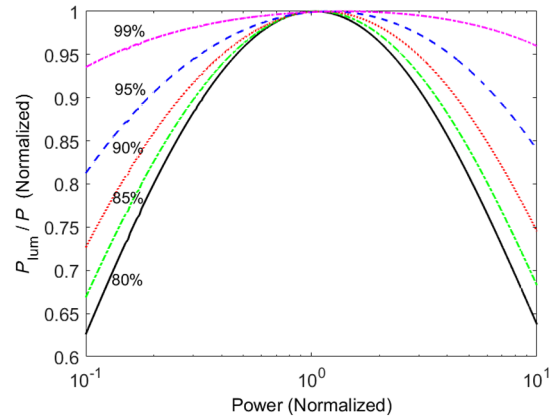


Fig. 1 Pulsed-PDPL theoretical curve for different optimum EQE.

$$\alpha I \Delta t = h\nu N_0, \quad (7)$$

where α is the resonant absorption coefficient, I is the incident pump intensity, Δt is the incident pulse duration, h is Planck's constant, and ν is the incident optical frequency. Since incident pump power $P = IA$, where A is the pump spot area, $P \propto N_0$.

We plot P_{lum}/P as a function of P (pump power) for different optimum EQE in Fig. 1. After normalizing to the peak of the curve, plots for different EQE values show different slopes before and after the peak. We then can use this feature to obtain the value of $\eta_{\text{ext}}^{\text{opt}}$ by comparing the experimental data with the theoretical curve.

3 Experiment and Results

The experimental setup is shown in Fig. 2. The optical pump source is a miniature diode-pumped Q-switched Er:YAG laser (1535 nm) (Photop Technologies, Model: DPQL-1535-C-0040-005N-03) frequency doubled to 767 nm using a KTP crystal. It delivers ~ 3.5 ns (full width at half maximum) pulses having $\sim 0.6 \mu\text{J}$ energy at 1 kHz repetition rate. Reference power and luminescence are collected by two identical photodetectors. The pump light is modulated with a rotating half-wave plate at ~ 1.5 Hz followed by a polarizing beamsplitter to obtain nearly 3 orders of magnitude of extinction ratio. A neutral density filter wheel is placed in front of the pump source to adjust the power to obtain data points on both sides of the peak on the pulsed-PDPL curve.

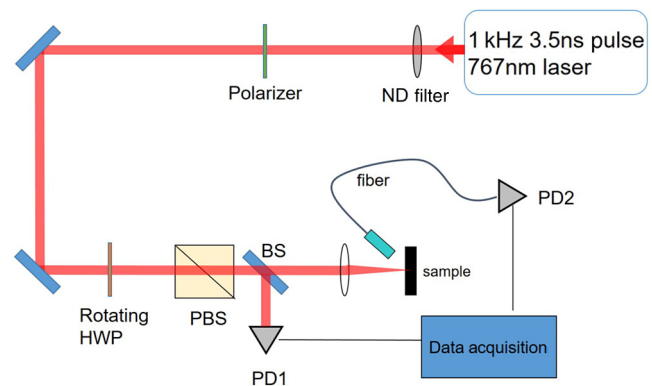


Fig. 2 Experimental setup for pulsed-PDPL.

Signals from both photodetectors are sent to an oscilloscope. The pulse stream for one cycle (or half cycle) of the modulation is then recorded and the peak signals of each pulse are picked out by a numerical algorithm using MATLAB. The ratio of the peak signals from two detectors is then plotted against the peak signals (incident power) of the reference detector (PD1).¹⁶

Figure 3 shows the room-temperature pulsed-PDPL experimental data for four different samples with different EQE values and the corresponding theoretical curves. All samples in Fig. 3 are ~1-mm diameter GaInP/GaAs/GaInP (750 nm/750 nm/750 nm) double heterostructures (DHS) lifted off from the GaAs substrate and Van der Waals bonded to 5-mm diameter ZnS hemispheres.¹⁷ The heterostructure wafers are grown by metal-organic chemical vapor deposition (MOCVD) or molecular beam epitaxial (MBE). The experimental data match theoretical curves very well. The uncertainty of EQE in this pulsed-PDPL experiment is about $\pm 1\%$ to $\pm 2\%$. We compare the EQE of these samples under the same condition by two different techniques (ASLC and pulsed-PDPL). The results are summarized in Table 1. The relative value agrees with each other, while pulsed-PDPL consistently gives smaller EQE than ASLC. The discrepancy can be attributed to the density dependence of radiative recombination coefficient B and the peak detection method used in data processing, both of which will be discussed later.

Table 1 Comparison of EQE measured by ASLC and pulsed-PDPL under the same condition on bonded samples at room temperature. DHS wafers are grown by MOCVD or MBE at three different institutions: Center for High Technology Materials (CHTM) at the University of New Mexico (UNM), Sandia National Laboratories (SNL), and National Renewable Energy Laboratory (NREL). Pulsed-PDPL data are given in Fig. 3.

Wafer	Growth method	Grown at	EQE by pulsed-PDPL on bonded samples (%)	EQE by ASLC (%)
A	MOCVD	SNL	90	94
B	MBE	CHTM (UNM)	78	82
C	MOCVD	SNL	85	86
D	MOCVD	NREL	89	92

In striking contrast to the ASLC technique, pulsed-PDPL can be used to easily screen samples without complicated and time-consuming fabrication processes and lens bonding. We perform pulsed-PDPL on several DHS samples with substrate (before processing). Figure 4 shows the experimental data for two samples at room temperature and the corresponding theoretical curves. The complete results are summarized in Table 2 for comparison with EQE obtained

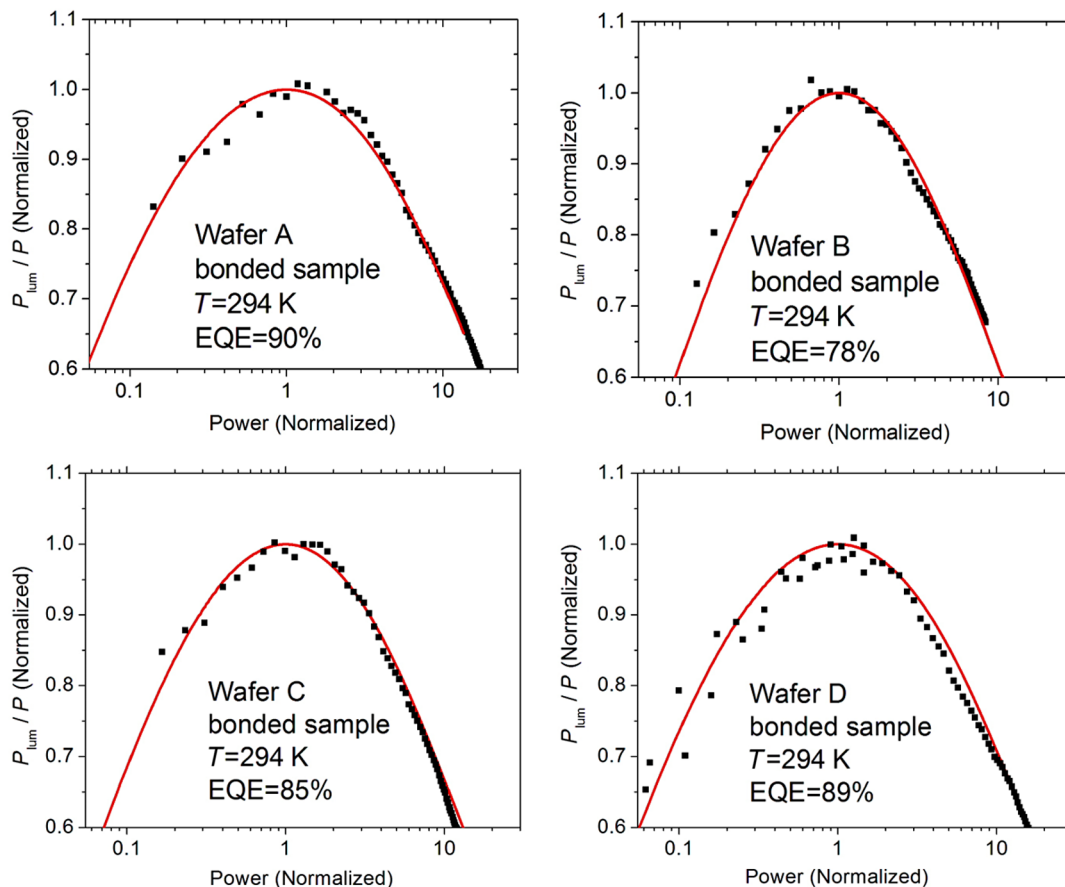


Fig. 3 Experimental data of pulsed-PDPL experiment on bonded samples at room temperature (dots). The solid lines are theoretical curves with fitting parameter of EQE = 90%, 78%, 85%, and 89%, respectively. The uncertainty of this technique is about $\pm 1\%$.

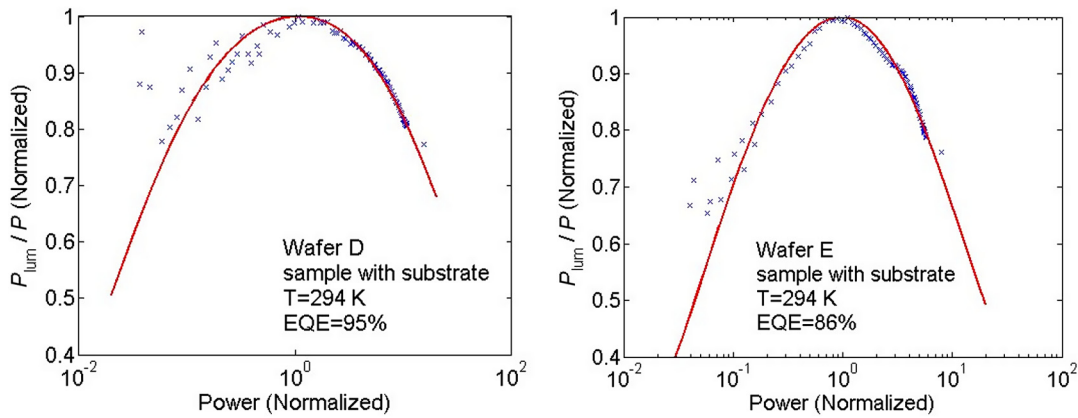


Fig. 4 Experimental data of pulsed-PDPL experiment (dots) on samples with substrate at room temperature. The solid lines are theoretical curves with fitting parameter of EQE = 95% and 86%, respectively.

Table 2 Comparison of EQE measured by ASLC on bonded samples and pulsed-PDPL on samples with substrates under the same condition at room temperature. Pulsed-PDPL data for wafers D and E are given in Fig. 4; pulsed-PDPL data for wafer A are given in Fig. 7.

Wafer	Growth method	Grown at	EQE by pulsed-PDPL on sample with substrate (%)	EQE by ASLC (%)
A	MOCVD	SNL	95	94
D	MOCVD	NREL	95	92
E	MOCVD	NREL	86	73.4

from ASLC on bonded samples from the same wafer. The EQE number obtained from PDPL on the sample with substrates shows the same trend but is consistently higher than the EQE obtained from ASLC on bonded samples, which is expected since the existence of the substrate will increase the extraction efficiency of the DHS sample and thus increase EQE. The summarized data show that, in general, pulsed-PDPL is an accurate tool to predict the EQE and to screen the sample effectively before processing.

A measurement of EQE at low temperatures is important for laser cooling in semiconductors since low starting

temperatures provide more favorable conditions to achieve net cooling.⁶ Therefore, we also perform pulsed-PDPL measurement at low temperatures. However, the data at low temperatures cannot be explained completely by the analytical solution of Eqs. (5) and (6) for the following reasons. First, radiative recombination coefficient B is a function of carrier density; second, the peak detection method used in the data processing is different from integrating the photoluminescence over infinite time as used in Eq. (6). Both factors have a stronger influence at low temperatures. Therefore, we simulate the problem numerically at low temperatures.

The density and temperature dependence of the B coefficient can be explained as follows. According to the plasma theory of Huang and Koch,¹⁸ the density and temperature dependence of resonant absorption coefficient α result from both Coulomb screening and band-blocking (saturation) effects. The latter can be approximated by a blocking factor such that¹⁹

$$\alpha(\nu, N, T) = \alpha_0(\nu) \{f_v - f_c\}. \tag{8}$$

The strong density-dependent blocking factor in the brackets contains Fermi–Dirac distribution functions for the valence (f_v) and conduction (f_c) bands. Using the “non-equilibrium” van Roosbroeck–Shockley relation, the luminescence spectral density R is related to the resonant absorption coefficient¹⁹

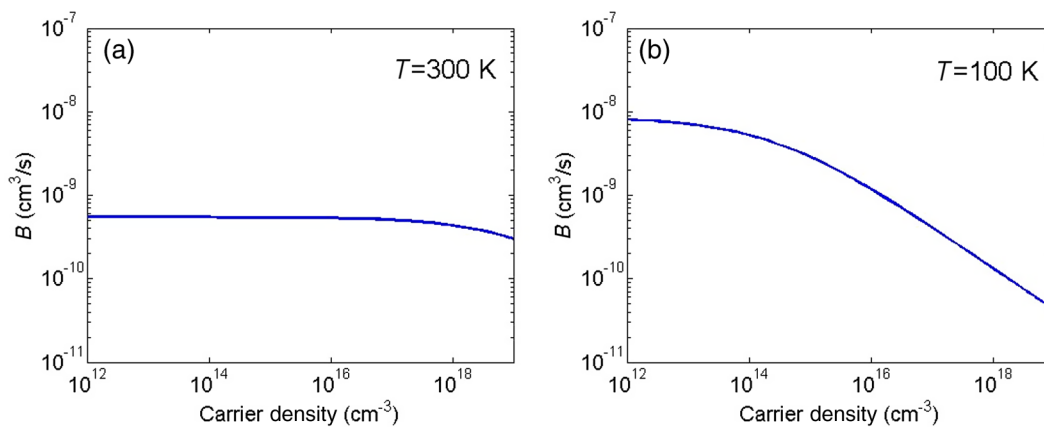


Fig. 5 Density-dependent B coefficient at (a) 300 K and (b) 100 K used to fit the pulsed-PDPL measurement data.

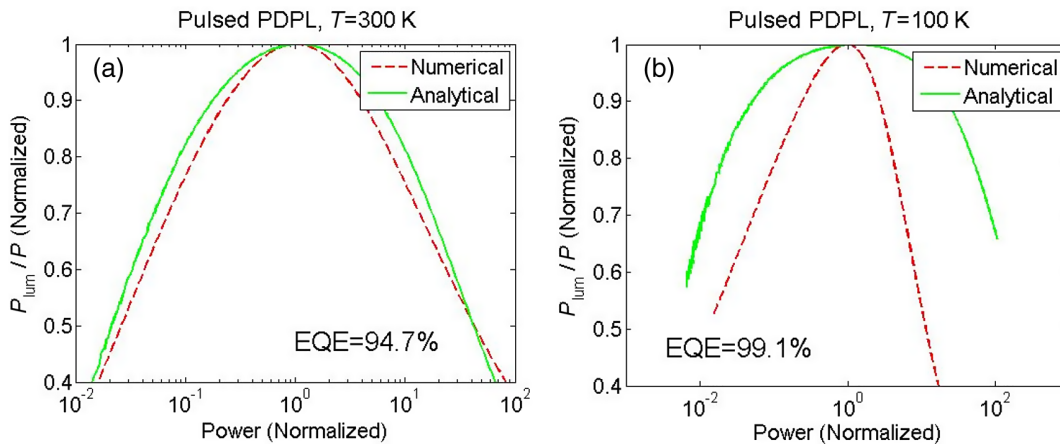


Fig. 6 Calculated pulsed-PDPL curve from analytical solution (green) using Eqs. (5) and (6) and from numerical simulation (red dashed) at (a) 300 K and (b) 100 K. The numerical simulation takes into account three effects: density-dependent radiative recombination, luminescence peak detection affected by detector rise time, and the pulse shape of the incident laser.

$$R(\nu, N, T) = \frac{8\pi n^2 \nu^2}{c^2} \alpha(\nu, N, T) \left\{ \frac{f_c(1-f_v)}{f_v - f_c} \right\}, \quad (9)$$

$$B(N, T) \approx \frac{5.5 \times 10^{-10} (300/T)^{2.5}}{1 + 3.9 \times 10^9 \sqrt{N} (300/T)^5}. \quad (10)$$

where c is the speed of light and n is the index of refraction.

Note that the radiative recombination coefficient B is obtained by $BN^2 = \int R(\nu) d\nu$, which results in a dependence of B on N at high carrier densities.

For our application, we use an empirical form for the temperature and density-dependent B coefficient¹⁶

The parameters in this empirical equation are determined by fitting it with the pulsed-PDPL data at various temperatures. Equation (10) is plotted in Fig. 5 for 300 and 100 K.

Figure 5 shows a stronger dependence of the B coefficient on carrier density at low temperature. Rupper et al.²⁰ have studied the density dependence of the B coefficient using different models of rigorous microscopic theory. Their result is consistent with our empirical form plotted in Fig. 5.

To reflect the peak detection method used in actual data collection, we calculate the time-dependent detector signal using

$$V(t) = \int_0^t \text{PL}(t') e^{-\frac{t-t'}{\tau}} dt', \quad (11)$$

where $\text{PL}(t')$ is the time-dependent photoluminescence signal calculated from Eq. (5) and τ is the detector rise time. We then find the maximum (peak) value of $V(t)$.

Figure 6 shows the results for both the numerical simulation and analytical solution at room temperature and 100 K under the same conditions. Note that the numerical results also consider the pulse shape of the incident laser while the analytical solution assumes a delta-function pulse. The results at 300 K show very little difference, indicating that our previous fit using an analytical solution is generally valid at room temperature. If using numerical simulation instead at room temperature, the obtained optimum EQE value will be slightly higher than the ones obtained from analytical equations, which explains the discrepancies we observed earlier. The results, however, differ a lot at 100 K, warranting the use of numerical simulation at low temperatures.

Figure 7 shows the experimental data at 100 K, 200 K and room temperature for one cooling sample before processing and the corresponding numerical simulation curve. They match very well and the obtained EQE values are, in general, consistent with ALS measurement at low temperatures on the same sample.

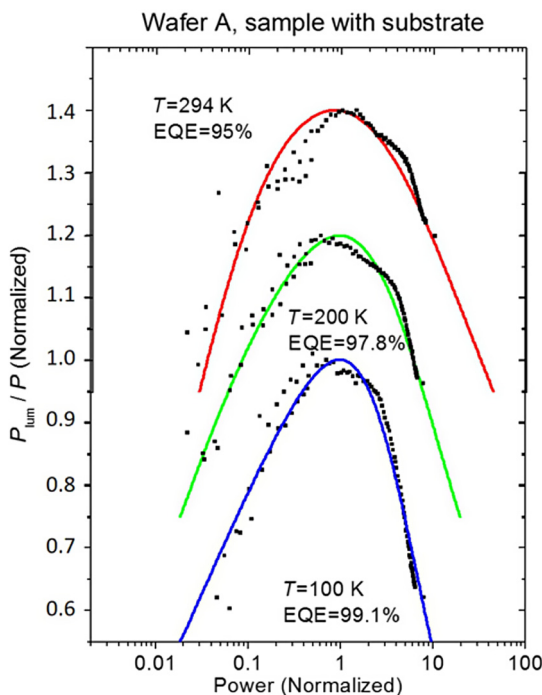


Fig. 7 Experimental data of pulsed-PDPL experiment (dots) on samples with substrate at different temperatures. The solid lines are simulation curves with fitting parameter of EQE = 99.1% at 100 K (blue), 97.8% at 200 K (green), and 95% at 294 K (red), respectively. Data are offset vertically for clarity.

4 Conclusion

In conclusion, pulsed-PDPL is developed as a rapid measurement for EQE in semiconductor materials. This technique is proven to be an accurate and efficient tool to screen samples before fabrication for the application of laser refrigeration of semiconductors.

Acknowledgments

This work was supported by the National Science Foundation Award DMR-1207489, AFOSR Grant FA9550-15-1-0241, AFRL Contract FA94531310223, AFOSR STTR Grant FA9550-13-C-0006, and DARPA STTR grant in collaboration with Thermodynamic Films LLC. We also thank Jeff Cederberg (Sandia National Laboratories, Albuquerque, New Mexico), Jerry Olson (National Renewable Energy Laboratory, Golden, Colorado), and Andreas Stintz (The University of New Mexico, Albuquerque, New Mexico) for the growth of the heterostructure samples.

References

1. O. Miller, E. Yablonovitch, and S. Kurtz, "Strong internal and external luminescence as solar cells approach the Shockley–Queisser limit," *IEEE J. Photovoltaics* **2**(3), 303–311 (2012).
2. M. Sheik-Bahae and R. I. Epstein, "Optical refrigeration," *Nat. Photonics* **1**, 693–699 (2007).
3. R. I. Epstein et al., "Observation of laser induced fluorescent cooling of a solid," *Nature* **377**, 500–503 (1995).
4. D. V. Seletskiy et al., "Laser cooling of solids to cryogenic temperatures," *Nat. Photonics* **4**, 161–164 (2010).
5. S. D. Melgaard et al., "Solid-state optical refrigeration to sub-100 Kelvin regime," *Nat. Sci. Rep.* **6**, 20380 (2016).
6. M. Sheik-Bahae and R. I. Epstein, "Can laser light cool semiconductors?," *Phys. Rev. Lett.* **92**(24), 247403 (2004).
7. J. Zhang et al., "Laser cooling of a semiconductor by 40 Kelvin," *Nature* **493**, 504–508 (2013).
8. D. Bender et al., "Development of high quantum efficiency GaAs/GaInP double heterostructures for laser cooling," *Appl. Phys. Lett.* **102**, 252102 (2013).
9. I. Schnitzer et al., "Ultrahigh spontaneous emission quantum efficiency, 99.7% internally and 72% externally, from AlGaAs/GaAs/AlGaAs double heterostructures," *Appl. Phys. Lett.* **62**, 131 (1993).
10. D. J. Dunstan, "On the measurement of absolute radiative and non-radiative recombination efficiencies in semiconductor lasers," *J. Phys. D* **25**, 1825–1828 (1992).
11. T. H. Gfroerer, E. A. Cornell, and M. W. Wanlass, "Efficient directional spontaneous emission from an InGaAs/InP heterostructure with an integral parabolic reflector," *J. Appl. Phys.* **84**, 5360 (1998).
12. K. R. Catchpole et al., "High external quantum efficiency of planar semiconductor structures," *Semicond. Sci. Technol.* **19**, 1232–1235 (2004).
13. H. Gauck et al., "External radiative quantum efficiency of 96% from a GaAs/GaInP heterostructure," *Appl. Phys. A*, **64**, 143–147 (1997).
14. C. Wang et al., "Precision, all-optical measurement of external quantum efficiency in semiconductors," *J. Appl. Phys.* **109**, 093108 (2011).
15. C. Wang et al., "GaAs/GaInP double heterostructure characterization for laser cooling of semiconductors," *Proc. SPIE* **7951**, 79510D (2011).
16. C. Wang, "Precise characterization and investigation of laser cooling in III–V compound semiconductors," PhD Dissertation, University of New Mexico (2015).
17. B. Imangholi et al., "Effects of epitaxial lift-off on interface recombination and laser cooling in GaInP/GaAs heterostructures," *Appl. Phys. Lett.* **86**, 081104 (2005).
18. H. Huang and S. W. Koch, *Quantum Theory of the Optical and Electronic Properties of Semiconductor*, World Scientific, Singapore (1990).
19. P. K. Basu, *Theory of Optical Processes in Semiconductors: Bulk and Microstructures*, Oxford University Press, New York (1997).
20. G. Rupper, N. H. Kwong, and R. Binder, "Optical refrigeration of GaAs: theoretical study," *Phys. Rev. B* **76**, 245203 (2007).

Chengao Wang received his PhD in optical science and engineering at the University of New Mexico in 2015. From 2013 to 2014, he was a senior engineer at Sumitomo Electric Device Innovations, USA. Currently, he is an R&D manager at Actoprobe, LLC. His research interests have included laser cooling of semiconductors, high-speed vertical cavity surface emitting lasers, optically pumped semiconductor lasers, and nonlinear optics.

Mansoor Sheik-Bahae obtained his PhD from SUNY-Buffalo in 1987 and spent seven years at CREOL (University of Central Florida) as a research professor. He is a distinguished professor of physics and astronomy at the University of New Mexico. His research interests have included nonlinear optics, ultrafast phenomena, semiconductor photonics, and laser cooling of solids. He is a fellow of OSA and was corecipient of OSA's R.W. Wood Prize in 2012.